nature cell biology

# Nuclear transport factor directs localization of protein synthesis during mitosis

Geert van den Bogaart[1,2,3], Anne C. Meinema[1,3], Victor Krasnikov[2], Liesbeth M. Veenhoff[1,4] and Bert Poolman[1,2,4]

**Export of messenger RNA from the transcription site in the nucleus and mRNA targeting to the translation site in the cytoplasm are key regulatory processes in protein synthesis. In yeast, the mRNA-binding proteins Nab2p and Nab4p/Hrp1p accompany transcripts to their translation site, where the karyopherin Kap104p mediates both their dissociation from the mRNA and their transport back into the nucleus. We found that Kap104p localized to the distal bud tip and the bud neck during cell division, resulting in a localized release of translation-competent mRNA and increased protein synthesis in the emerging daughter cell. Temporally and spatially coordinated localization of Kap104p is a new mechanism for the asymmetric distribution of protein synthesis in dividing cells.**

During its maturation, mRNA is complexed with a changing repertoire of proteins, a fraction of which act co-transcriptionally. These proteins are involved in the modification of mRNA, including 5′-end capping, splicing, 3′-end cleavage and poly(A) addition, and only fully processed transcripts are exported from the nucleus[1]. In addition to mRNA processing, a complex of proteins bound to a single mRNA, called messenger ribonucleoprotein (mRNP), also regulates the export, targeting, stability and translatability of the transcript[2–6]. Trafficking of mRNP to distinct cellular sites is a common mechanism for ensuring protein synthesis at defined subcellular sites, and it has been found to regulate cell polarity as well as asymmetry during development and differentiation in animals, plants and fungi[7].

The transport of molecules between the cytoplasmic and nuclear compartments occurs through nuclear pore complexes (NPCs)[8] and involves the formation of a carrier–cargo complex, translocation through the NPC, release of the cargo molecule at the *trans* side, and recycling of the carrier. Most nuclear transport involves the binding of a carrier of the β-karyopherin superfamily to a nuclear localization signal (NLS) present on the cargo. In contrast, mRNA export employs several proteins unrelated to karyopherins, such as the Mex67–Mtr2 heterodimer[2,3] and nuclear polyadenylated RNA-binding proteins 2 and 4 (Nab2p and Nab4p/Hrp1p). Nab2p is a protein related to human heterogeneous nuclear RNP (hnRNP) that binds poly(A) RNA with high affinity, as demonstrated by its dissociation constant of about 30 nM (refs 9–12). Nab2p is essential for mRNA export of a subset of transcripts, and its absence leads to the accumulation of poly(A) RNA in the nucleus[12–14]. Nab4p/Hrp1p is the yeast protein most similar in sequence to mammalian hnRNP A1. In addition to being a factor for the export of mRNA, Nab4p is a component of the cleavage factor I complex[15]. Another abundant mRNP component is poly(U)-binding protein (Pub1p). In the cytoplasm, the bulk of Nab2p interacts directly with Pub1p, and this interaction modulates transcript stability[16]. Before translation, Nab2p and Nab4p are released from the mRNA. The binding of cytosolic karyopherin Kap104p (Kapβ2/Trn in metazoans) to the NLSs of Nab2p (rgNLS) and Nab4p has been implicated in this release[9,17–19]. The release of Nab2p from the mRNA is also mediated by the ADP-bound form of the DEAD-box RNA helicase Dbp5p[12]. After the release of Nab2p and Nab4p, the Kap104–cargo complex is imported into the nucleus, where RanGTP and mRNA act cooperatively to dissociate both Nab2p and Nab4p from Kap104p, probably resulting in only a small fraction of Nab2p not being bound to mRNA or Kap104p[9].

Because of its function as a nuclear transport factor, Kap104p was expected to be uniformly distributed in the cytoplasm. We determined the subcellular localization of Kap104p in a *Saccharomyces cerevisiae* strain that produces a carboxy-terminally tagged Kap104p–GFP (green fluorescent protein) from the genomic *KAP104* locus. Surprisingly, Kap104p–GFP accumulated roughly 10-fold compared with the cytoplasm at the distal tip of the daughter cell during early mitotic phase of the cell cycle (referred to hereafter as M phase) and about 50-fold at the bud neck during late M phase; that is, at and after nuclear division (Fig. 1a–c; Supplementary Information, Movie S1). Kap104p was the only one of the 14 known karyopherins in yeast that localized to the bud neck or distal tip (not shown). A FRAP (fluorescence recovery after photobleaching) study indicated that Kap104p–GFP was still mobile at the bud neck and the bud tip, with a half time of recovery ($t_{1/2}$) of 4–8 s (Fig. 1d). The cytoplasmic concentration of Kap104p–GFP during G1 phase (no bud present) was about 1 μM (Fig. 1e) as determined from the fluorescence intensity, which corresponds to about 25,000 mol-

[1]Department of Biochemistry, University of Groningen, Nijenborgh 4, 9747 AG, Groningen, The Netherlands. [2]Zernike Institute for Advanced Materials, University of Groningen, Nijenborgh 4, 9747 AG, Groningen, The Netherlands.
[3]These authors contributed equally to this work
[4]Correspondence should be addressed to L.M.V. or B.P. (e-mail: l.m.veenhoff@rug.nl; b.poolman@rug.nl)

Received 14 October 2008; accepted 11 November 2008; published online 8 February 2009; DOI:10.1038/ncb1844

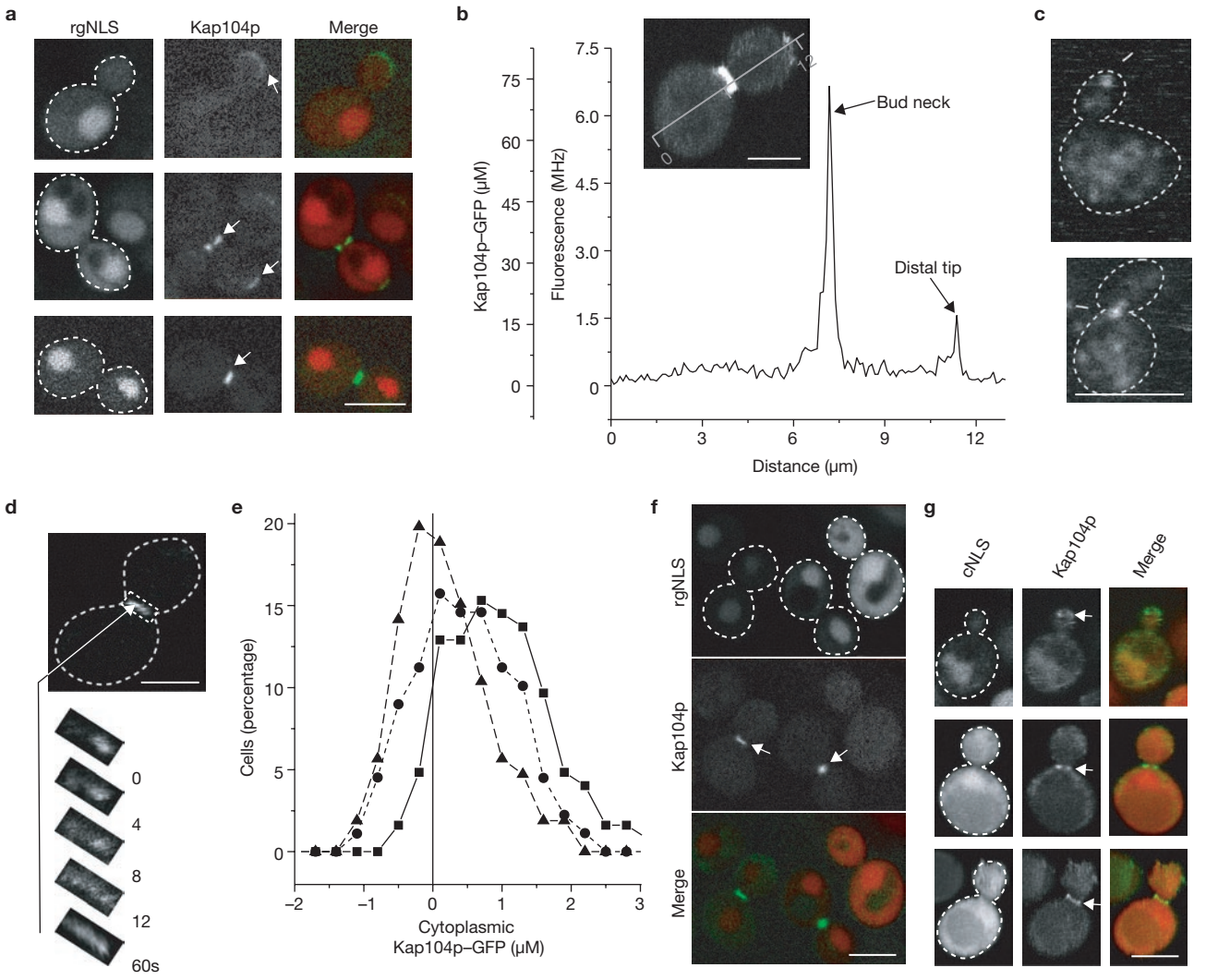


**Figure 1** Kap104p localizes to the distal tip and to the bud neck in M phase. (**a**) Confocal images of three budding yeast cells expressing chromosomal GFP-tagged Kap104p (Kap104p–GFP, white arrows) and the rgNLS–mCherry reporter expressed from a plasmid. The merged images show Kap104p–GFP in green and rgNLS–mCherry in red. Dashed lines indicate the contour of the cells. (**b**) The distribution of Kap104p–GFP in the yeast cell shown in the inset (track indicated by the grey line). The concentration of Kap104p–GFP was estimated by quantitative western blotting, and from the fluorescence intensity, by using FCS on cell extracts (Supplementary Information, Fig. S1). (**c**) Cells stained with Alexa fluor 633-labelled antibodies directed against Kap104p. (**d**) FRAP experiment indicating that Kap104p in the bud neck diffuses with a $t_{1/2}$ of 4–8 s. (**e**) The distribution of cytoplasmic Kap104p–GFP concentration in 124 cells with no apparent bud (G1 phase, squares, solid line) and in 89 cells with a bud (S/M phase, circles, dotted line). The estimated Kap104p–GFP concentration was corrected for autofluorescence (triangles, dashed line; 0 μM, 106 cells, strain BY4742). (**f**) Three mitotic cells with different levels of expression of rgNLS–mCherry. The approximate cytoplasmic concentrations of rgNLS–mCherry are 0.13 μM (left), 1.2 μM (middle) and 9.7 μM (right); the experiment shows that rgNLS–mCherry can displace Kap104p–GFP from the bud neck. (**g**) High expression of the Kap95p/60p-targeted SV40 cNLS fused to mCherry from a plasmid did not result in displacement of Kap104p–GFP from the bud neck. The approximate cytoplasmic concentrations of cNLS–mCherry were 0.8 μM (top), 6.2 μM (middle) and 10.5 μM (bottom). Scale bars, 5 μm.

ecules per cell and agrees well with the quantitative western analysis (Supplementary Information, Fig. S1) and previous data[20]. During M phase, the free cytoplasmic concentration of Kap104p–GFP decreased to about 0.5 μM. Introduction of a multi-copy plasmid-encoding mCherry or GFP bearing the NLS from Nab2p (rgNLS–mCherry or rgNLS–GFP, respectively) gave rise to a population of cells containing a variable number of copies of the gene and resulted in a wide range of expression levels of the reporter. We used this characteristic to determine whether the binding of Kap104p to the bud neck or bud tip and the binding of Kap104p–cargo are competitive events. Indeed, in cells expressing rgNLS-tagged mCherry[21] at cytoplasmic concentrations greater than 5 μM, Kap104p–GFP did not accumulate in the distal bud tip or bud neck (Fig. 1f). A control experiment in which the rgNLS was replaced with the Kap60p/95p-targeted simian virus 40 (SV40) did not result in displacement of Kap104p–GFP from the bud neck (Fig. 1g), indicating that the competition was specific for Kap104p–cargo.

Next we addressed the nucleocytoplasmic transport of the Kap104p-targeted rgNLS–mCherry reporter throughout the cell cycle. We found that the localization of Kap104p to the distal tip and later to the bud neck coincided with a decrease in Kap104p-mediated accumulation of nuclear rgNLS–mCherry relative to cytoplasmic rgNLS–mCherry, the NC ratio (Fig. 2a–c). The total amount of reporter present in a cell remained roughly the same during the cell cycle. The NC ratio of the rgNLS reporter is a result of active import and passive efflux through the

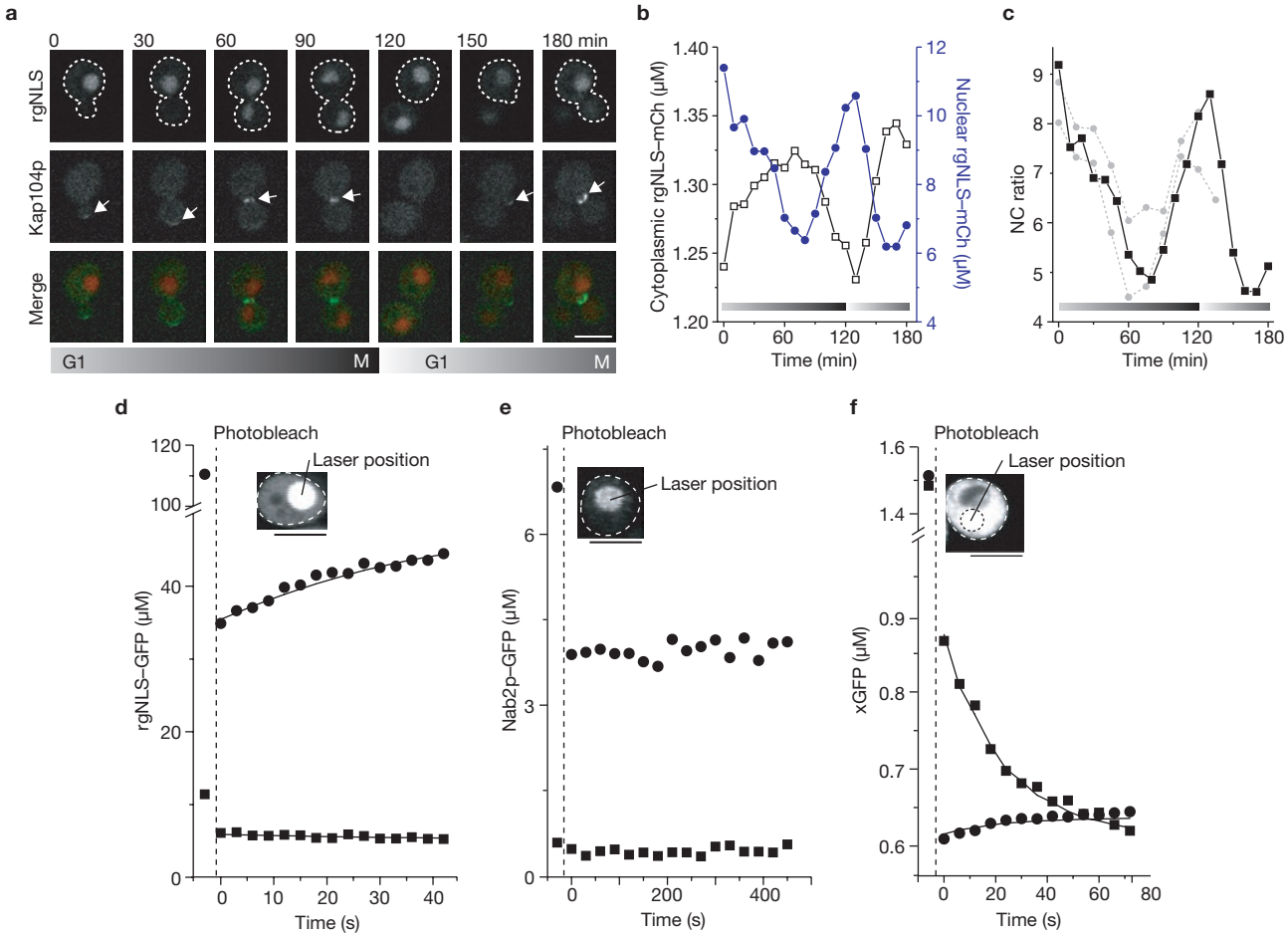


**Figure 2** Kap104p localization to the distal tip and bud neck coincides with decreased nuclear import. (**a**) Time series of confocal images of yeast cells expressing chromosomal GFP-tagged Kap104p (Kap104p–GFP, white arrows) and the rgNLS–mCherry reporter expressed from a plasmid. The merge of the two images is also shown (green, Kap104p–GFP; red, rgNLS–mCherry) The succession of the cell cycle phases is shown underneath the corresponding panels (G1, M). (**b**) Concentrations of the rgNLS–mCherry (rgNLS–mCh) reporter in the cytoplasm (open squares, left axis) and the nucleus (blue filled circles, right axis) for the budding cell from **a**. (**c**) The NC ratios of the rgNLS–mCherry reporter, calculated from the concentrations from **b** (filled squares, solid line). For comparison, results for two other budding cells are also shown (grey filled circles, dotted lines). (**d**) Selective FRAP was used to determine the transport rates of the rgNLS–GFP reporter through the nuclear pore complex. First, the laser was focused for about 5–10 s on the nucleus of a yeast cell expressing rgNLS–GFP (inset). This resulted in the photobleaching of part of the GFP located in the nucleus (circles) and the cytoplasm (squares) and a deviation from the steady-state NC ratio. The relaxation of the NC ratio as a result of the net import of intact GFP and the net efflux of photobleached GFP was followed by recording of a time series of images. The solid lines present a fit with equation (2) (Methods); the import and efflux rates were 2.9 and 0.2 molecules $s^{-1}$ per NPC per μM of substrate, respectively. (**e**) As in **d**, but for chromosomally GFP-tagged Nab2p (Nab2p–GFP). Relaxation did not occur within 10 min. (**f**) As in **d**, but for GFP not fused to a NLS (xGFP). This 29-kDa molecule is small enough to diffuse passively through the NPC[20] and is uniformly distributed over the nucleus and the cytoplasm (NC ratio = 1). As both import and efflux follow the same diffusion-mediated process we expect them to be the same; indeed, the import and efflux rates were both 1.3 molecules $s^{-1}$ per NPC per μM of substrate. Scale bars, 5 μm.

NPC[20]. Efflux of this small (33.1 kDa) reporter is substantial but several-fold slower than active import. The Kap104p-mediated nuclear import rate has been reported to be limited by the association of karyopherin with cargo and to depend linearly on the cytoplasmic concentration of Kap104p[20]. Indeed, on a typical halving of the cytoplasmic concentration of Kap104p in M phase (Fig. 1e), we observed a similar decrease in the Kap104p-mediated nuclear accumulation of the rgNLS reporter (Fig. 2a-c). To determine the kinetics of Kap104p-mediated nucleocytoplasmic transport, we developed a FRAP-based assay. Selective FRAP (reviewed in ref. 22) is based on the partial (about 40%) photobleaching of fluorophores in a cellular compartment and monitoring of the subsequent import of non-bleached fluorophores. We modified the assay to measure nucleocytoplasmic transport quantitatively in yeast (Fig. 2d–f). For Kap104p-mediated import of rgNLS–GFP, relaxation typically occurred within 40–60 s (Fig. 2d). An import rate of 2.1 ± 0.7 $s^{-1}$ per NPC per μM of substrate was determined; the efflux rate was 0.23 ± 0.17 $s^{-1}$ per NPC per μM of substrate. In contrast, under identical conditions, relaxation of Nab2p–GFP to the steady-state NC ratio did not occur within 10 min after photobleaching (Fig. 2e). We were unable to quantify the rates of entry as well as exit from the nucleus, but they must be more than an order of magnitude lower than that of the rgNLS–GFP reporter. Existing literature reports that Nab2p is passed on directly from the mRNA to Kap104p in the cytoplasm, and vice versa in the nucleus[9,17–19]. Taking into account the fast kinetics of the actual Kap104p-mediated import cycle, for example with rgNLS–GFP, our data therefore indicates that most of the Nab2p–GFP signal is reflecting Nab2p bound to mRNA, and, once released from the mRNA, Nab2p is quickly removed from the cytoplasm by import into the nucleus. Because Nab2p dissociates from

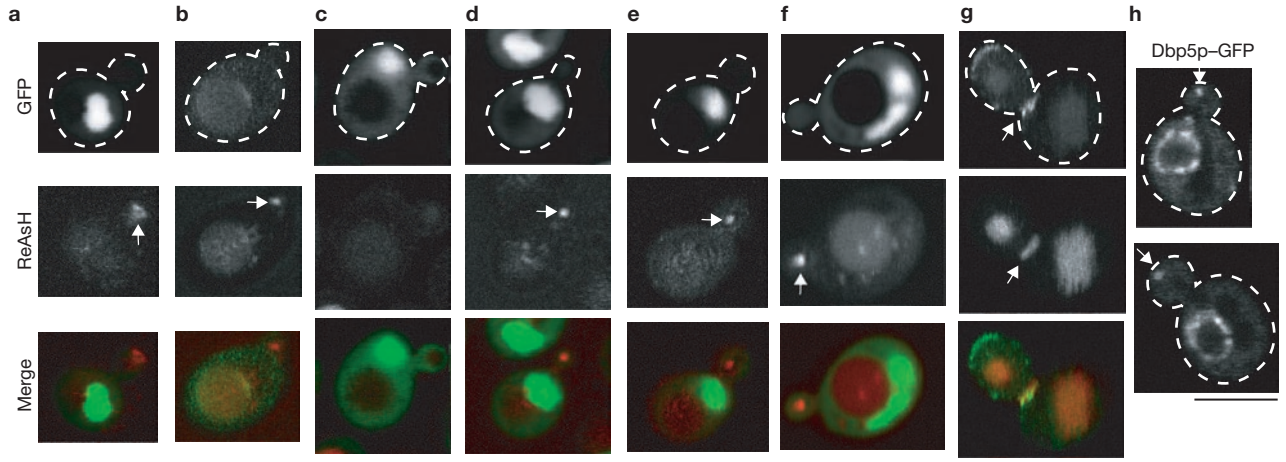


**Figure 3** Asymmetric distribution of translation sites. (**a**) Cycloheximide-treated cell expressing the rgNLS–GFP reporter with N-terminal tetracysteine (TC) domain for labelling with ReAsH (rgNLS-TC–GFP, NC ratio = 7.7 ± 0.6 s.e.m.) For 40 out of 62 budding cells that were imaged, the ReAsH-stained translation sites were more abundant in the daughter cells (white arrow). (**b**) As in **a**, but with the SV40 NLS C-terminal to the GFP (TC–GFP–cNLS), instead of the rgNLS; the asymmetry in the translation sites was observed for 30 out of 48 cells imaged. Generally, because of the lower nuclear accumulation of the cNLS (NC ratio = 3.2 ± 0.4 (ref. 20)), the nuclear GFP signal of TC–GFP–cNLS was less than that of the rgNLS-TC–GFP reporter. (**c**) As in **a**, but for the temperature-sensitive Kap104p mutant[18] at the non-permissive temperature (1.5 h at 37 °C). No ReAsH-stained translation sites were visible in the bud (NC ratio = 3.2 ± 0.3); a lack of ReAsH-stained translation sites in the bud was observed in all cells imaged ($n = 31$). (**d**, **e**) Control experiments with the temperature-sensitive Kap104 mutant at 30 °C (**d**, NC ratio = 7.9 ± 0.7) and with the wild-type strain at 37 °C (**e**, NC ratio = 7.6 ± 0.7); 31 out of 42 and 29 out of 51 cells, respectively, showed the ReAsH-stained translation sites in the bud. (**f**) As in **a**, but using the *she2*Δ deletion mutant; 23 out of 31 cells showed translation sites in the bud. (**g**) The TC–MBP–cNLS reporter was used to resolve Kap104–GFP and protein localization (ReAsH staining) simultaneously. In a small fraction of cells (4 out of 40), the ReAsH signal was still present in the distal tip or bud neck and overlapped the Kap104p localization (white arrows). (**h**) A substantial fraction of Dbp5p–GFP localized to the distal tip during M phase (white arrows), and the rest to the nuclear envelope. Scale bar, 5 μm.

the mRNA before translation[17] and because fluorescence *in situ* hybridization (FISH) experiments indicated that the total amount of mRNA was uniformly distributed over the mother and daughter cells (Supplementary Information, Fig. S2; ref. 23), we predicted that the asymmetric distribution of Kap104p could impose asymmetric protein synthesis by enriching translation-competent mRNA in the bud; that is, after transfer of Nab2p from mRNA to Kap104p. To test this hypothesis, we determined the translational activity in live cells.

An rgNLS-TC–GFP reporter protein was expressed with the tetracysteine motif (TC) located amino-terminal to GFP[24]. The TC motif can bind specifically to the non-fluorescent, cell-envelope-permeable, biarsenical labelling reagent ReAsH, thereby forming a fluorescent complex. Fully translated rgNLS-TC–GFP protein is imported into the nucleus. Because the TC domain is translated first, ReAsH can bind to the nascent chain as it emerges from the ribosome. Furthermore, inhibition of translation elongation by cycloheximide results in increased ribosome packing of the mRNA[25]. Indeed, treatment with cycloheximide resulted in specific, concentrated bright red ReAsH staining located primarily in the bud (Fig. 3a; Supplementary Information, Fig. S3). For cycloheximide-treated cells, the ReAsH signal emerging from the translation sites was more than tenfold that from the nucleus, where ReAsH was bound to the mature reporter protein. Replacing the rgNLS with the Kap60p/95p-targeted SV40 cNLS showed that the localization was independent of the NLS (Fig. 3b). Kap104p was necessary for localized translation in the bud, because the concentrated ReAsH staining was absent from the temperature-sensitive Kap104 mutant (*Kap104-16*; ref. 18) at the non-permissive temperature (37 °C; Fig. 3c). Under these conditions Kap104 protein levels decreased, as is apparent from the decreased nuclear accumulation of the rgNLS reporter. Control experiments with the temperature-sensitive strain at the permissive temperature (30 °C) and the wild-type strain at 37 °C (Fig. 3d, e) confirm that loss of ReAsH staining was due to depletion of Kap104p. The determining role of Kap104p in localized protein synthesis is supported further by the observation that asymmetry in translation sites was not observed in cells expressing the cytoplasmic rgNLS reporter at concentrations above 5 μM, in which Kap104p was displaced from the distal bud tip or bud neck (Fig. 1f). The mechanism of localized translation is independent of the She pathway of mRNA targeting, because deletion of the gene encoding the She2p RNA-binding protein[26] did not result in an altered localization of the translation sites (Fig. 3f).

The ReAsH assay is complicated by the fact that the treatment with cycloheximide, needed to increase the ribosome packing, resulted in diminished localization of Kap104p to the distal tip and bud neck. To permit simultaneous visualization of Kap104p–GFP and the ReAsH translation sites, we replaced GFP in the TC reporter by a maltose-binding protein (MBP). Importantly, in most cycloheximide-treated cells, most Kap104p no longer localized to the distal tip cortex but formed a punctate staining that overlapped with the ReAsH signal in the daughter cell. In a small fraction of the cells, clear ReAsH signals were still observed at the cortex of the distal tip and the bud neck (Fig. 3g). Taken together, these results indicate that in budding yeast, translation does indeed colocalize with Kap104p and takes place at the distal tip and bud neck. More recently, it was shown that Dbp5p mediates the dissociation of Nab2p from mRNA[12], and 40–60% of total Dbp5p has been found associated with mRNA-polyribosome complexes[27]. Interestingly, a substantial fraction of a GFP-tagged version of Dbp5p also localized to the distal tip (Fig. 3h) and presumably associates with the translation sites.

The hypothesis of localized protein synthesis, taken together with the transport data, implies the fast removal of Nab2p from the cytoplasm once released from the mRNA, and would lead to an asymmetric distribution of Nab2p over mother and bud in those stages of the cell-cycle

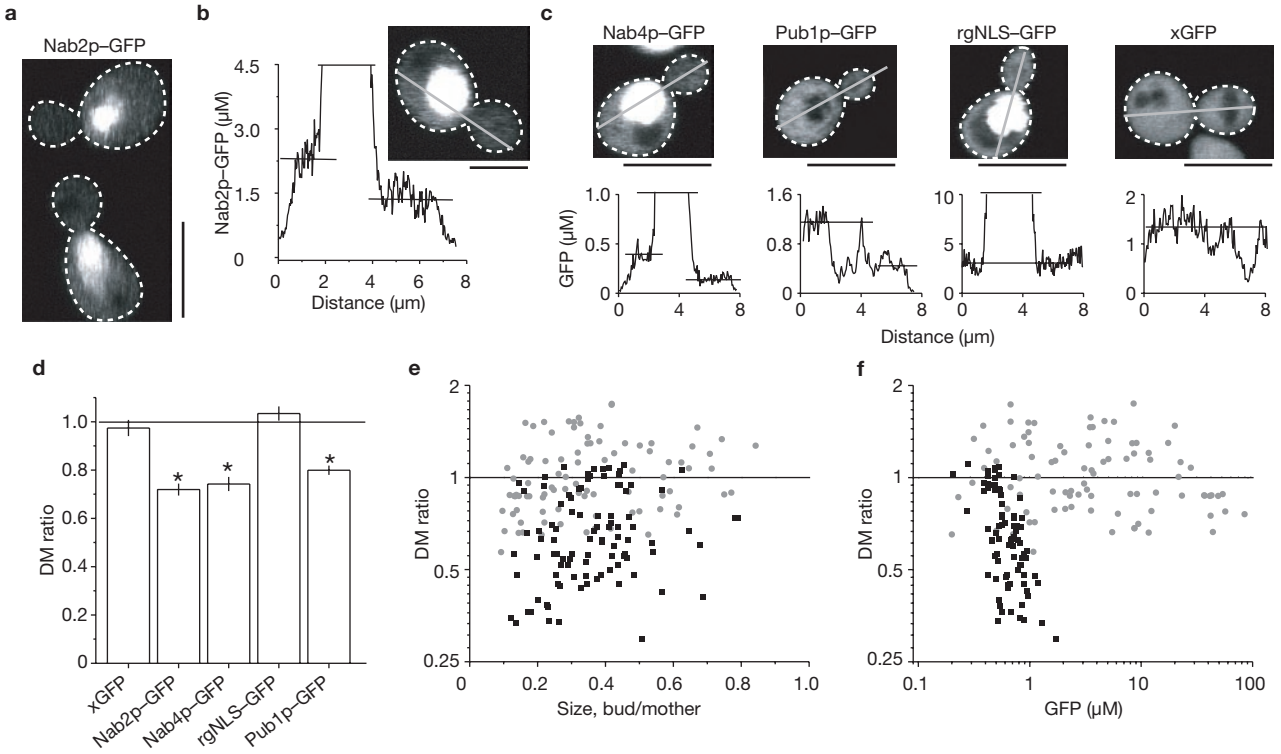


**Figure 4** Nab2p shows a lower cytoplasmic concentration in the emerging daughter than in the mother cell. (**a**) Confocal image of budding yeast cells expressing chromosomal GFP-tagged Nab2p. (**b**) Nab2p–GFP distribution (dashed lines) of the yeast cell shown in the inset (track indicated by the grey bar). (**c**) As in **b**, but for yeast cells expressing chromosomally GFP-tagged Nab4p (Nab4p–GFP) or Pub1p (Pub1p–GFP), also showing lower cytoplasmic concentrations in the bud. Cells expressing plasmid-encoded GFP with (rgNLS–GFP) or without (xGFP) fusion to the rgNLS showed a symmetric distribution over mother and bud. Scale bars, 5 μm. (**d**) The average ratio of the concentrations in bud and mother (DM ratio) of more than 50 budding cells expressing xGFP, Nab2p–GFP, Nab4p–GFP, rgNLS–GFP or Pub1p–GFP. Error bars indicate s.e.m.; asterisk, significantly deviation of the ratio from that of xGFP (*t*-test; $P < 0.05$). (**e**) DM ratio plotted as a function of the size of the bud relative to that of the mother for Nab2p–GFP (squares, $n = 101$) and rgNLS–GFP (grey circles, $n = 91$). There was no significant correlation (Spearman's rank, $P < 0.01$) for both datasets, indicating that the asymmetrical distribution is not an artefact arising from the diffraction-limited axial resolution. (**f**) DM ratio as a function of cytoplasmic concentration in the mother cell of Nab2p–GFP (squares) and rgNLS–GFP (grey circles). There was a significant negative correlation between Nab2p–GFP and DM ratio; no correlation was found for rgNLS–GFP.

in which Kap104p localized to the bud. Indeed, during M phase, concentrations of Nab2p–GFP expressed from the genomic *NAB2* locus were 20–30% lower in the bud than in the mother cell (Fig. 4a, b). It is possible that the real concentration difference is higher. Quantification was difficult as a result of low expression levels, resulting in fluorescence intensities that were close to autofluorescence. Similar observations were made for chromosomal, GFP-tagged versions of the Kap104–cargo Nab4p and of the cytoplasmic Nab2p interaction partner Pub1p. The lower Nab2p, Nab4p and Pub1p levels in the bud are not an artefact of the imaging method, because GFP without a NLS (xGFP) and rgNLS–GFP were distributed equally over mother and bud (Fig. 4c, d). In addition, there was no apparent correlation between the size of the bud and the ratio of the cytoplasmic GFP concentration in the bud relative to the mother cell (Fig. 4e), which would have been the case if the result was an artefact resulting from the diffraction limited axial resolution. Our hypothesis also predicts that the asymmetry of the Nab2p distribution should be highest when Kap104p localizes to the bud. We used the cytoplasmic concentration of Nab2p–GFP to report the cell cycle stage because the cytoplasmic Nab2p–GFP is high when import is low as a result of Kap104p localization to the bud (Fig. 2a–c). Indeed, a significant negative correlation was found between the cytoplasmic concentration of Nab2p–GFP and its asymmetric distribution (Fig. 4f). In other words, in cells with a higher cytoplasmic Nab2p–GFP concentration, the Nab2p–GFP distribution was more asymmetric.

In summary, we have made the following observations. Kap104p is localized in the distal tip of the daughter cell during early M phase and to the bud neck during late M phase. This apparent partitioning coincides with a decrease in Kap104p-mediated nucleocytoplasmic transport and with decreased levels of Nab2p and Nab4p in the bud. The transport kinetics are consistent with the association of the vast majority of cytoplasmic Nab2p and Nab4p with mRNPs. During M phase, translation of the transcripts coding for the rgNLS-TC–GFP and TC–GFP–cNLS reporter proteins, and presumably many other proteins, is most prominent in the bud. The presence of functional Kap104p is essential for the localized translation.

On the basis of these data, we propose a simple model in which the localized Kap104p evokes enhanced protein synthesis in the newly forming daughter cell by freeing mRNA from associated proteins. During G1 phase (Fig. 5a), Kap104p is uniformly distributed in the cell and the dissociation of Nab2p and Nab4p from mRNA takes place throughout the cytoplasm. Furthermore, Kap104p facilitates the translocation of Nab2p and Nab4p through the NPC. During early M phase (Fig. 5b), about 50% of Kap104p and about 10–20% of Dbp5p become localized to the distal tip of the daughter cell. Therefore, dissociation of Nab2p and Nab4p from mRNA and fast re-import of the Nab proteins into the nucleus will

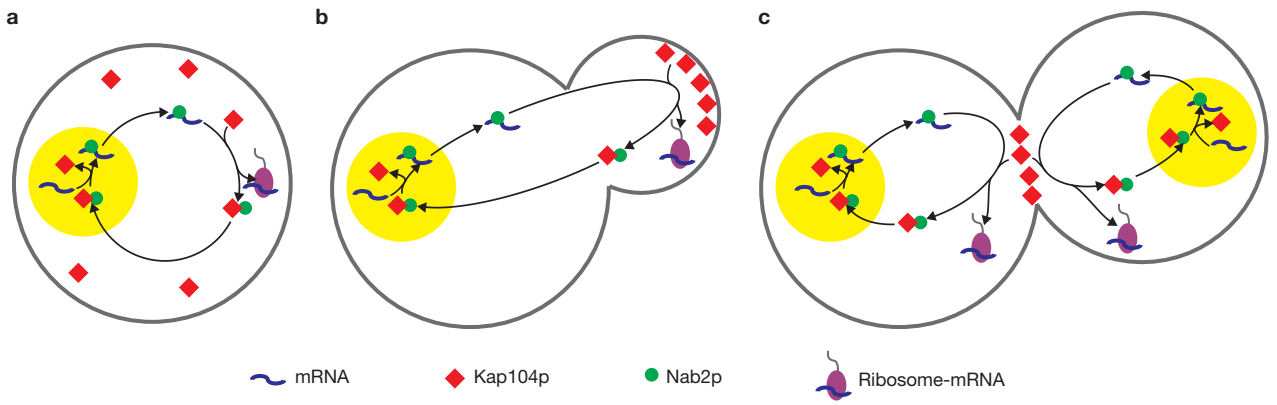


**Figure 5** Model of Kap104p-mediated mRNA targeting. Nab2p binds to mRNA in the nucleus (yellow), and this complex is translocated to the cytoplasm, where Kap104p and/or Dbp5p mediate the dissociation of Nab2p from the mRNA, allowing translation. The Kap104p–Nab2p complex returns to the nucleus by means of Ran-driven nucleocytoplasmic transport. (**a**) During G1 phase, Kap104p is uniformly distributed over the cell, and the dissociation of Nab2p from the transcripts occurs throughout the entire cytoplasm. (**b**) During early M phase, Kap104p (and Dbp5p) locate to the distal tip, resulting in localized Nab2p dissociation (and re-import into the nucleus) and localized mRNA translation. (**c**) In late M phase, Kap104p localizes to the bud neck. We propose that this localization tunes the distribution of mRNA and associated proteins over the mother and daughter cells, allowing the daughter cell to mature to full size.

take place mainly in the bud, resulting in a decrease in the cytoplasmic concentrations of Nab2p and Nab4p in the daughter cell relative to the mother cell. The unloading of Nab2p mediated by Kap104p and Dbp5p, and presumably the co-release of translational repressors at the distal tip, thus effectively target translation-competent mRNA to the emerging daughter cell. The position of Kap104p switches to the bud neck during late M phase (Fig. 5c). If Kap104p in the bud neck were to release roughly half of the transcripts for the daughter and half for the mother cell, it could still have a decisive role in cell growth, because the volume of the daughter cell is about 50% (diameter about 80%) that of the mother during cytokinesis. The distinct localization of Kap104p in the bud neck might also relate to its role in cell cycle progression and regulation of mitotic exit[28]. The mechanism of subcellular Kap104p localization is still unclear, but many kinases involved in cell cycle progression locate to the bud neck. Especially interesting is the finding that Hrr25p, a kinase catalysing a mitosis-specific phosphorylation on nucleoporin Nup53p, shows a localization pattern similar, although not identical, to that of Kap104p, first to the bud and later to the bud neck[29].

Specific mRNA localization[7] is a crucial step in the control of local protein synthesis and is necessary for the establishment of cell polarity, asymmetric development and differentiation in higher eukaryotes. Using budding yeast as a model system, we report a novel mechanism by which cell-cycle-dependent localization of Kap104p effectively organizes the subcellular distribution and localization of translation-competent mRNA between the mother and the emerging daughter cell. □

## METHODS

**Plasmids and strains.** Plasmids and strains were obtained with conventional techniques, described in Supplementary Methods. All experiments were performed in yeast strain BY4742 (Invitrogen), grown in (low fluorescent) synthetic dropout medium complete (SDC) with or without histidine, uracil or leucine (pH 5.4; Sigma-Aldrich), supplemented with 2% (w/v) glucose. Expression of the TC–GFP–cNLS reporter was induced by growth overnight in synthetic dropout medium without histidine, supplemented with 2% (w/v) raffinose and 0.1% (w/v) galactose (no glucose).

**Microscopy.** Microscopy and selective FRAP were performed with a laser scanning confocal microscope, as described elsewhere[30]. Exponentially growing cells were kept in the SDC growth medium at 30 °C and immobilized under the microscope with poly-(L-lysine)-coated coverslips. The dwell times for laser scanning confocal microscopy were between 0.1 and 0.3 ms and the pixel steps were between 30 and 100 nm. For each of the images, a pixel analysis was used to determine the volumes and fluorescence intensities of the various cell compartments (nucleus and cytoplasm; Supplementary Information, Fig. S1). These intensities were converted into absolute GFP/mCherry concentrations, using the count rate per molecule estimated from fluorescence correlation spectroscopy (FCS) measurements on crude cell extracts. The fluorescence quantum yield in the cell extract was assumed to be similar to that in the cell. Immunofluorescence was performed as described in Supplementary Methods.

**Staining of translation sites with ReAsH.** The sites of translation were stained by using a similar approach to that described in ref. 25 and Supplementary Information, Fig. S3. Cells in the exponential phase of growth, expressing plasmid-encoded rgNLS-TC–GFP, rgNLS–GFP, TC–MBP–cNLS or TC–GFP–cNLS, were harvested by centrifugation (5,000*g* for 2 min) and concentrated twofold in SDC supplemented with 1 mg ml$^{-1}$ cycloheximide. After incubation for 30 min at 30 °C, the cell-permeable labelling reagent 4,5-bis(1,3,2-dithiarsolan-2-yl)-resorufin (ReAsH; Invitrogen) was added to a concentration of 5 μM and the cell suspension was incubated in the dark for 1 h at 30 °C. The cells were washed with 250 μM 2,3-dimercapto-1-propanol and concentrated tenfold in SDC supplemented with 1 mg ml$^{-1}$ cycloheximide for imaging. Control experiments were performed without cycloheximide treatment and with rgNLS–GFP (without the tetracysteine domain).

**Selective FRAP.** Selective FRAP, also called selective photobleaching (reviewed in ref. 22), was performed to determine the kinetics of nucleocytoplasmic transport. For selective FRAP, a confocal image of a yeast cell was recorded and the laser was focused on the nucleus for 5–10 s, resulting in partial (about 40–50%) photobleaching of the GFP (fused to the rgNLS or full-length Nab2p; Fig. 2d–f). As a result of the compact, barrel-like structure of GFP, it is shielded from the external environment and no damaging effects to the cell are caused by reactive intermediates generated by photobleaching[22]. Because nucleocytoplasmic transport still occurred during this photobleaching step, the signal from the cytoplasm was also decreased by about 20–30%. The NC ratio, defined as the ratio of the GFP concentration in the nucleus to that in the cytoplasm, was thus decreased by the selective photobleaching and subsequently recovered to the steady-state NC ratio by means of net nuclear import. The import of intact GFP was followed by recording a time series of images, using the same laser intensity as for photobleaching (less than 10 μW at the back aperture of the objective). Additional photobleaching during imaging was less than 3% and was neglected. The changes in the concentrations of GFP in the cytoplasm and the nucleus were fitted by

using a model based on the assumption that diffusion of GFP in the cytoplasm and nucleus is much faster than the import and efflux rates and therefore these rates depend linearly on the cytoplasmic and nuclear concentrations of GFP. For the concentration change in the nucleus,

$$\frac{dC_N(t)}{dt} = \frac{IC_C(t) - EC_N(t)}{A} \quad (1)$$

where $C_N(t)$ and $C_C(t)$ are the concentrations in the nucleus and cytoplasm, respectively; $I$ and $E$ are the influx and efflux rates and $A = V_N$, where $V_N$ is the volume of the nucleus. For the concentration change in the cytoplasm, the solution is similar but now $A = -V_C$, where $V_C$ is the volume of the cytoplasm. The analytical solution of equation (1) for $C_N(t)$ is given by

$$C_N(t) = B\frac{C_N(0)V_N + C_C(0)V_C}{EV_C + IV_N} + C\frac{EC_N(0) - IC_C(0)}{EV_C + IV_N}\exp\left[-\left(\frac{E}{V_N} + \frac{I}{V_C}\right)t\right] \quad (2)$$

where $B = I$, $C = V_C$ and $C_N(0)$ and $C_C(0)$ are the initial concentrations of GFP. For $C_C(t)$, the solution is similar, but now $B = E$ and $C = -V_N$. The rates from equation (2) were converted to the turnover of the NPC by assuming a constant density of 12 NPCs $\mu m^{-2}$, as reported in ref. 20. We found no effect of the photobleaching of GFP on the viability and growth of the cells.

*Note: Supplementary Information is available on the Nature Cell Biology website.*

**ACKNOWLEDGEMENTS**

We thank M. P. Rout, B. L. Timney, C. Strambio-de-Castillia, J. J. Schuringa, J. D. Aitchison and P. Orlean for strains, plasmids and valuable comments. Financial support was provided by the Netherlands Science Foundation NWO (ALW grant number 814.02.002; *VENI* fellowship to L.M.V.; TopSubsidy to B.P.), the Netherlands Proteomics Centre and the Zernike Institute for Advanced Materials.

**AUTHOR CONTRIBUTIONS**

Experimental work and data analysis: G.v.d.B., A.C.M. and L.M.V. Writing of manuscript: G.v.d.B., A.C.M., L.M.V. and B.P. Project planning: L.M.V. and B.P. Technical support: V.V.

**COMPETING FINANCIAL INTERESTS**

The authors declare that they have no competing financial interests.

Published online at http://www.nature.com/naturecellbiology
Reprints and permissions information is available online at http://npg.nature.com/reprintsandpermissions/

1. Bentley, D. L. Rules of engagement: co-transcriptional recruitment of pre-mRNA processing factors. *Curr. Opin. Cell Biol.* **17,** 251–256 (2005).
2. Köhler, A. & Hurt, E. Exporting RNA from the nucleus to the cytoplasm. *Nature Rev. Mol. Cell. Biol.* **8,** 761–773 (2007).
3. Stewart, M. Ratcheting mRNA out of the nucleus. *Mol. Cell* **25,** 327–330 (2007).
4. Lécuyer, E. *et al.* Global analysis of mRNA localization reveals a prominent role in organizing cellular architecture and function. *Cell* **131,** 174–187 (2007).
5. Isken, O. & Maquat, L. E. Quality control of eukaryotic mRNA: safeguarding cells from abnormal mRNA function. *Genes Dev.* **21,** 1833–1856 (2007).
6. Huang, Y. S. & Richter, J. D. Regulation of local mRNA translation. *Curr. Opin. Cell. Biol.* **16,** 308–313 (2004).
7. Müller, M., Heuck, A. & Niessing, D. Directional mRNA transport in eukaryotes: lessons from yeast. *Cell. Mol. Life Sci.* **64,** 171–180 (2007).
8. Macara, I. G. Transport into and out of the nucleus. *Microbiol. Mol. Biol. Rev.* **65,** 570–594 (2001).
9. Lee, D. C. & Aitchison, J. D. Kap104p-mediated nuclear import. Nuclear localization signals in mRNA-binding proteins and the role of Ran and RNA. *J. Biol. Chem.* **274,** 29031–29037 (1999).
10. Hector, R. E. *et al.* Dual requirement for yeast hnRNP Nab2p in mRNA poly(A) tail length control and nuclear export. *EMBO J.* **21,** 1800–1810 (2002).
11. Kelly, S. M. *et al.* Recognition of polyadenosine RNA by zinc finger proteins. *Proc. Natl Acad. Sci. USA* **104,** 12306–12311 (2007).
12. Tran, E. J., Zhou, Y., Corbett, A. H. & Wente, S. R. The DEAD-box protein Dbp5 controls mRNA export by triggering specific RNA:protein remodeling events. *Mol. Cell* **28,** 850–859 (2007).
13. Green, D. M. *et al.* Nab2p is required for poly(A) RNA export in *Saccharomyces cerevisiae* and is regulated by arginine methylation via Hmt1p. *J. Biol. Chem.* **277,** 7752–7760 (2002).
14. Guisbert, K., Duncan, K., Li, H. & Guthrie, C. Functional specificity of shuttling hnRNPs revealed by genome-wide analysis of their RNA binding profiles. *RNA* **11,** 383–393 (2005).
15. Gross, S. & Moore, C. Five subunits are required for reconstitution of the cleavage and polyadenylation activities of *Saccharomyces cerevisiae* cleavage factor I. *Proc. Natl Acad. Sci. USA* **98,** 6080–6085 (2001).
16. Apponi, L. H. *et al.* An interaction between two RNA binding proteins, Nab2 and Pub1, links mRNA processing/export and mRNA stability. *Mol. Cell. Biol.* **27,** 6569–6579 (2007).
17. Windgassen, M. *et al.* Yeast shuttling SR proteins Npl3p, Gbp2p, and Hrb1p are part of the translating mRNPs, and Npl3p can function as a translational repressor. *Mol. Cell. Biol.* **24,** 10479–10491 (2004).
18. Aitchison, J. D., Blobel, G. & Rout, M. P. Kap104p: a karyopherin involved in the nuclear transport of messenger RNA binding proteins. *Science* **274,** 624–627 (1996).
19. González, C. I., Ruiz-Echevarría, M. J., Vasudevan, S., Henry, M. F. & Peltz, S. W. The yeast hnRNP-like protein Hrp1/Nab4 marks a transcript for nonsense-mediated mRNA decay. *Mol. Cell* **5,** 489–499 (2000).
20. Timney, B. L. *et al.* Simple kinetic relationships and nonspecific competition govern nuclear import rates *in vivo*. *Cell. Biol.* **175,** 579–593 (2006).
21. Campbell, R. E. *et al.* A monomeric red fluorescent protein. *Proc. Natl Acad. Sci. USA* **99,** 7877–7882 (2002).
22. Goodwin, J. S. & Kenworthy, A. K. Photobleaching approaches to investigate diffusional mobility and trafficking of Ras in living cells. *Methods* **37,** 154–164 (2005).
23. Long, R. M. *et al.* Mating type switching in yeast controlled by asymmetric localization of ASH1 mRNA. *Science* **277,** 383–387 (1998).
24. Martin, B. R., Giepmans, B. N., Adams, S. R. & Tsien, R. Y. Mammalian cell-based optimization of the biarsenical-binding tetracysteine motif for improved fluorescence and affinity. *Nature Biotechnol.* **23,** 1308–1314 (2005).
25. Rodriguez, A. J., Shenoy, S. M., Singer, R. H. & Condeelis, J. Visualization of mRNA translation in living cells. *J. Cell Biol.* **175,** 67–76 (2006).
26. Paquin, N. & Chartrand, P. Local regulation of mRNA translation: new insights from the bud. *Trends Cell. Biol.* **18,** 105–111 (2008).
27. Gross, T. *et al.* The DEAD-box RNA helicase Dbp5 functions in translation termination. *Science* **315,** 646–649 (2007).
28. Asakawa, K. & Toh-e, A. A defect of Kap104 alleviates the requirement of mitotic exit network gene functions in *Saccharomyces cerevisiae*. *Genetics* **162,** 1545–1556 (2002).
29. Lusk, C. P. *et al.* Nup53p is a target of two mitotic kinases, Cdk1p and Hrr25p. *Traffic* **8,** 647–660 (2007).
30. Van den Bogaart, G., Hermans, N., Krasnikov, V., De Vries, A. H. & Poolman, B. On the decrease in lateral mobility of phospholipids by sugars. *Biophys. J.* **92,** 1598–1605 (2007).

nature cell biology



DOI: 10.1038/ncb1844

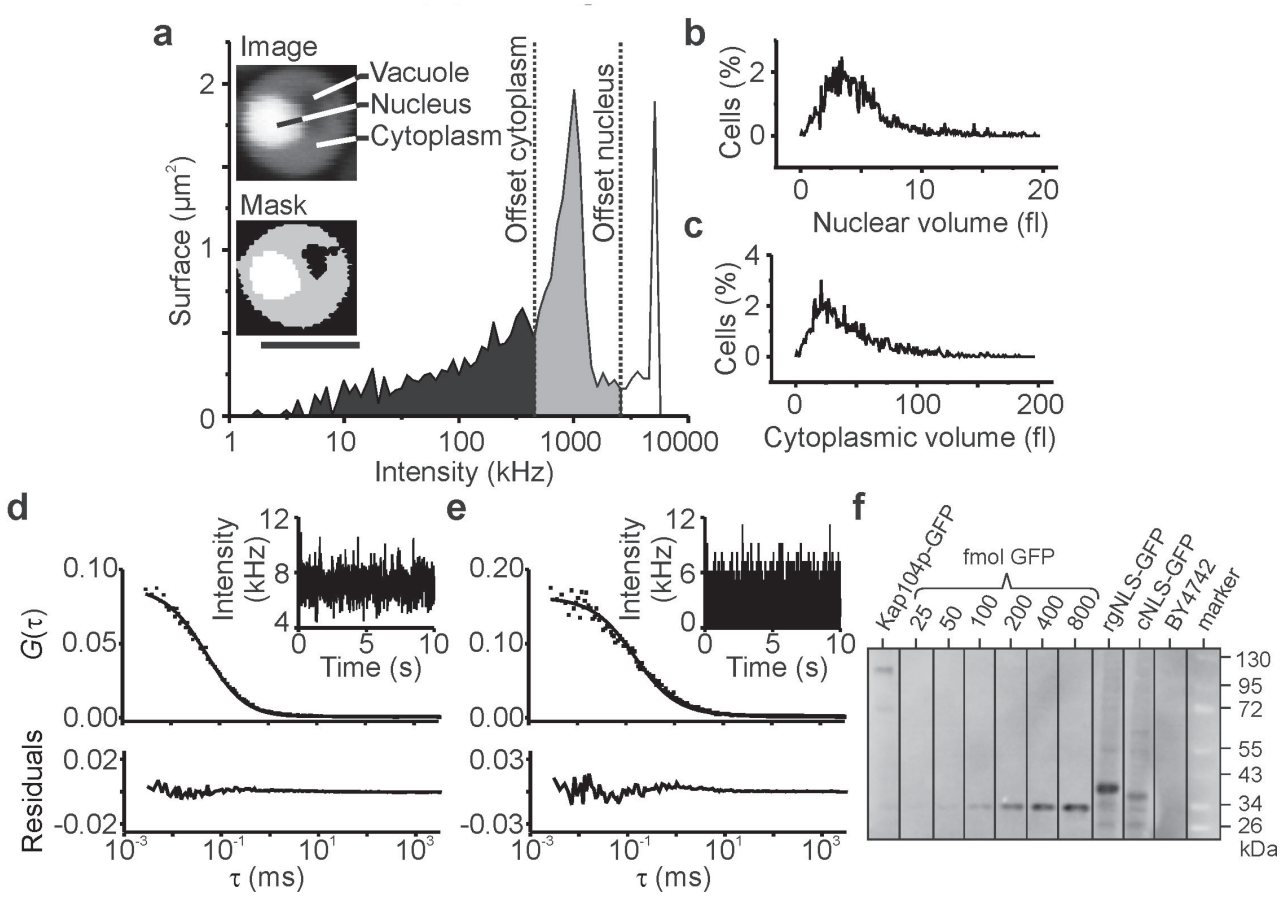


**Figure S1** Image analysis to determine the nuclear and cellular volumes and concentrations of GFP and mCherry. (**a**) The inset shows a confocal image of a yeast cell expressing a NLS fused to GFP (Image) and a mask overlay (Mask). This mask overlay was used for the fluorescence quantification and estimation of the cytoplasmic and nuclear volumes (panels b-c). Scale bar, 5 μm. The main figure presents the distribution of the fluorescence intensity in the background and vacuole (black), cytoplasm (grey) and nucleus (white). The peak intensities were used for the determination of the GFP concentrations, using the average count rate per molecule as determined with FCS on crude cell extracts (panels **d**-**e**), which were 12 μM and 62 μM for the cytoplasm and nucleus of this cell, respectively. For the conversion, the fluorescence quantum yield in the cell extract was assumed to be similar to that in the cell. The number of bins was kept at 75 for the various images, with the highest intensity $I_H$ in the last bin and a logarithmic bin-width of $\log(I_H) / 75$. (**b**-**c**) Distributions of the volumes of the nucleus (b, 4.3 ± 2.0 fl) and the cytoplasm (**c**, 44.3 ± 19.2 fl) of 1733 yeast cells and with bin-widths of 0.1 and 1 fl, respectively. The volumes were determined from the confocal images (panel a), using 3-dimensional morphometry, and by assuming that the shape of the cell, the vacuole and the nucleus is spherical. Using this method, the volumes differed < 10% from those calculated using more sophisticated topologies and multiple confocal slices [Timney, *et al.* (2006) *J. Cell. Biol.* **175**:579-593, Winey, *et al.* (1997) *Mol. Biol. Cell.* **8**:2119-2132]. (d) FCS measurement (▪) and fit (solid line) on a cell-free lysate from yeast cells expressing GFP. The residuals from the fit are presented in the lower graph and the fluorescence trace in the inset. The number of particles was 11.5 ± 1.8, the diffusion constant was 82 ± 14 $\mu m^2 s^{-1}$ and the count-rate per molecule was 0.75 ± 0.08 kHz $molecule^{-1}$. The focal volumes for the green and red channels of our setup are ~0.2 fl and ~0.45 fl, respectively [Veldhuis, *et al.* (2006) *Protein Sci.* **15**:1977-1986]. (**e**) Same as panel d, but now for a cell-free lysate of mCh. The number of particles was 5.7 ± 0.9, the diffusion constant was 79 ± 8 $\mu m^2 s^{-1}$ and the count-rate per molecule was 0.33 ± 0.04 kHz $molecule^{-1}$. (**f**) Quantitative Western blot analysis. Cells were grown to $10^7$ cells $ml^{-1}$, washed and lysed by boiling the cell suspensions for 5 min in 100 mM Tris HCl, pH 7.5, supplemented with 1% SDS. Subsequently, 0.7 g $ml^{-1}$ glass beads (0.1 mm diameter) were added, and the samples were shaken twice in a FastPrep device (Bio101, Vista, CA) for 20 s at force 6. Cell lysates were cleared by centrifugation for 2 min at 20,000 ×g. For each of the cell samples, the equivalent of $2 \times 10^6$ cells were loaded on the SDS-PAGE gel. The amounts of GFP-fusion protein in the cell lysates was determined using Western blot analysis with a primary antibody raised against GFP (Sigma-Aldrich, St Louis, MO). His-tagged GFP purified from *Escherichia coli* was used for calibration. The amounts of protein were 40,000 copies/cell for Kap104p-GFP (~1.5 μM), 80,000 copies/cell for cNLS-GFP (~3 μM), and 150,000 copies/cell for rgNLS-GFP (~6 μM).

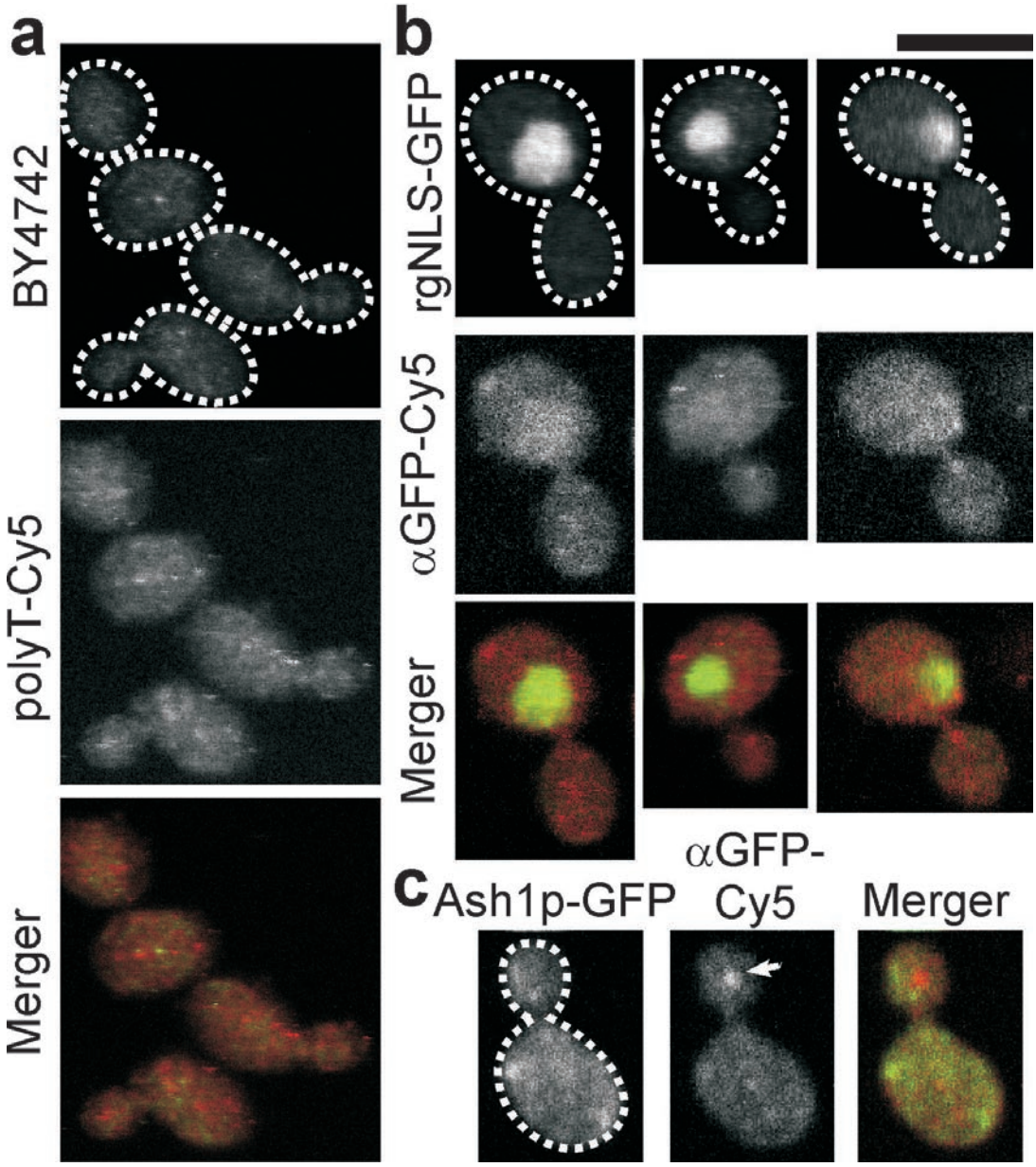


**Figure S2** Fluorescence *in situ* hybridization (FISH) in mitotic yeast cells. RNA was stained by FISH using a protocol from http://www.singerlab.org/protocols and adapted from [Long, *et al.* (1995) *RNA* **1**:1071-1078]. (**a**) FISH in BY4742 cells probed with polyT-Cy5 (5'-Cy5-oligo d(T)21, Gene Link, Hawthorne, NY) did not show a asymmetric cytoplasmic distribution of polyadenylated mRNA over the mother and the emerging daughter cell. The hybridization of the polyT-Cy5 oligonucleotide was performed in 15% formamide. (**b**) FISH in cells expressing the rgNLS-GFP reporter and probed with a Cy5-labeled oligonucleotide against transcripts encoding for GFP did not show a asymmetric cytoplasmic distribution of mRNAs coding for rgNLS-GFP over the mother and the daughter cell (αGFP-Cy5; (5'-(Cy5) CTCCG GTGAA GGTGA AGGTG ATGCT ACTTA C, Sigma-Aldrich, St. Louis, MO)). The hybridization of the αGFP-Cy5 oligonucleotide was performed in 50% formamide. (**c**) Positive control for the αGFP-Cy5 probe. Cells that express a C-terminal GFP-fusion of Ash1p from the genomic *ASH1* locus show an accumulation of the GFP encoding transcripts in the daughter cell (white arrow) [Paquin N, Chartrand P (2008) *Trends Cell. Biol.* **18:**105-111]. Scale bar, 5 μm.

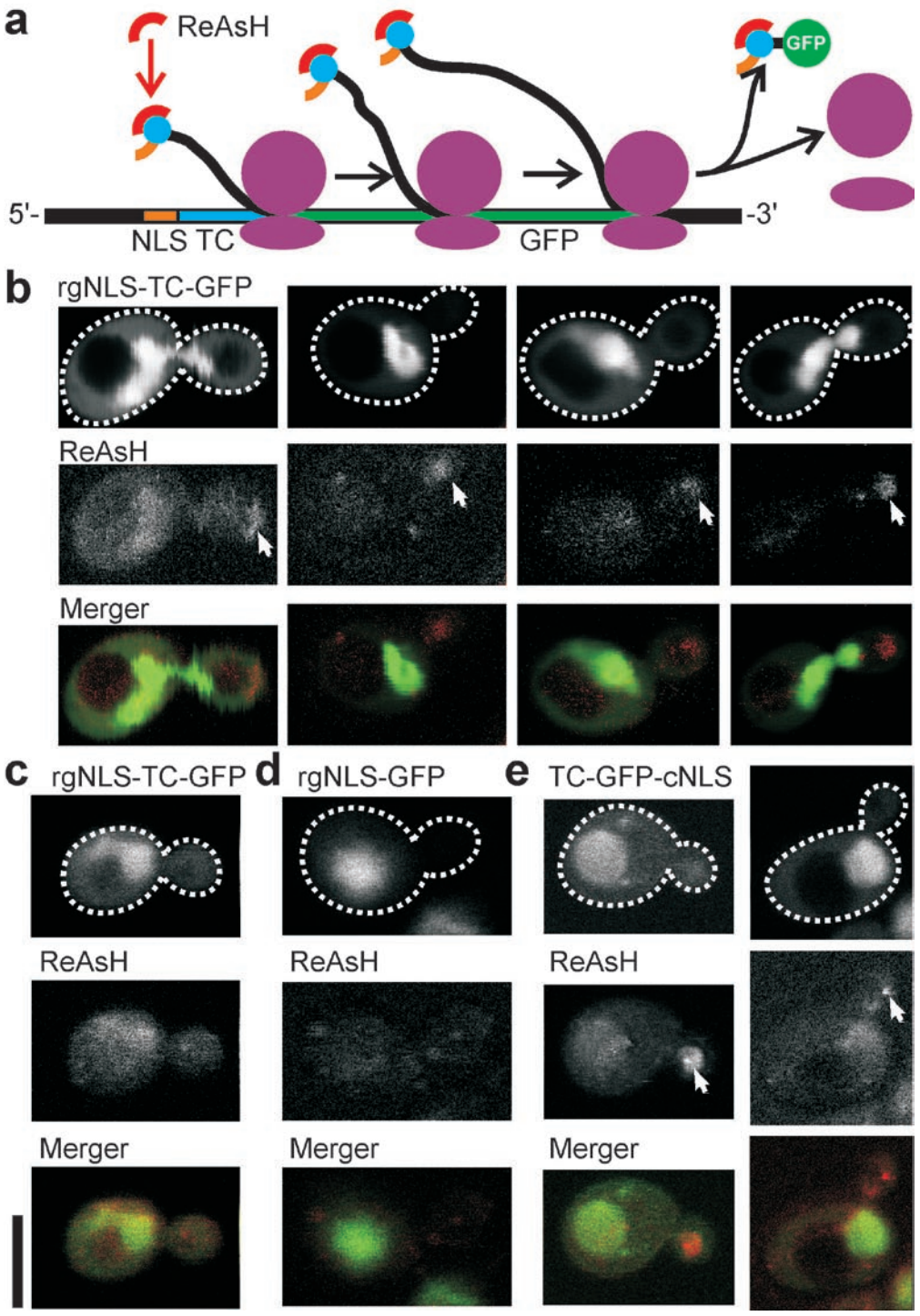


**Figure S3** Increased translation in the emerging daughter cell. (**a**) Cartoon of the ReAsH staining of the translation sites, adapted from [Rodriguez, *et al.* (2006) *J. Cell. Biol.* **175**:67-76]. The rgNLS-TC-GFP reporter protein was expressed with the tetracysteine motif located N-terminal of the GFP. The TC motif can bind specifically to the non-fluorescent, cell permeable [Andresen, *et al.* (2004) *Mol. Biol. Cell.* **15**:5616-5622], biarsenical labeling reagent ReAsH, thereby forming a fluorescent complex. The completed rgNLS-TC-GFP protein is imported into the nucleus. Because the TC domain is translated first, ReAsH can already bind to the nascent chain while emerging from the ribosome. Inhibition of translation elongation by cycloheximide results in increased ribosome packing of the mRNA and bright red, punctate ReAsH-staining of the sites of translation. (**b**) ReAsH and cycloheximide-treated cells expressing the rgNLS-TC-GFP reporter. Note that the ReAsH-stained translation sites are much more abundant in the daughter cell (white arrows); four typical cells are shown. (**c**) Same as panel b, but now without cycloheximide-treatment. The concentrated bright red ReAsH-stained sites of translation were less apparent and the signals for ReAsH and rgNLS-TC-GFP overlapped. (**d**) Same as panel b, but without the TC-domain present (rgNLS-GFP). No ReAsH-staining of the nucleus or translation sites was observed. (**e**) Same as panel b, but now for cells expressing the TC-GFP-cNLS construct. Scale bar, 5 μm.

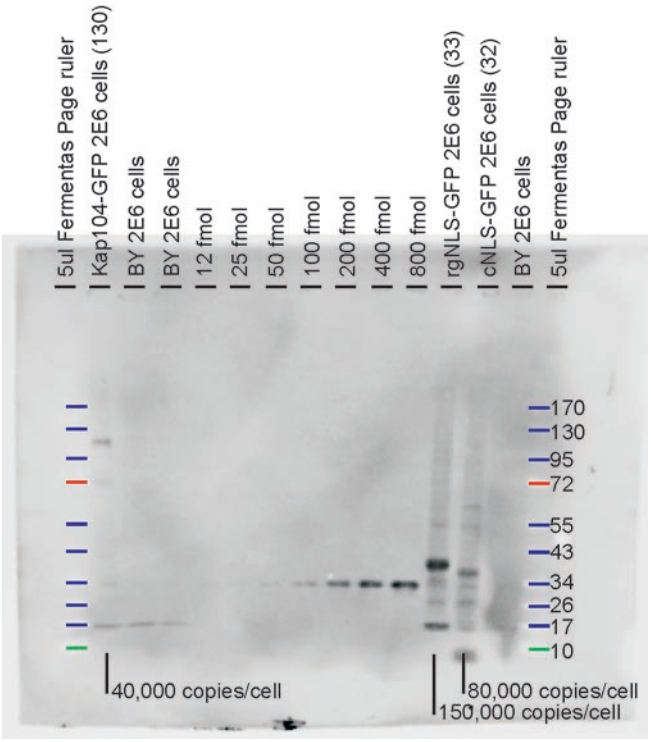


**Figure S4** Full scan of western in SI-figure 1f.

**Movie S1** Budding yeast cells expressing Kap104p-GFP (green) from the *KAP104* locus and the rgNLS-mCherry reporter expressed from a plasmid (red).

## Supplementary information, Methods S1

### Plasmids and strains

The construct coding for rgNLS-GFP was obtained by removing the PrA coding sequence from pBT016Nab2NLSGFPPrA [Timney, *et al.* (2006) *J. Cell. Biol.* **175**:579-593], using restriction enzymes *Hind*III and *Xho*I and ligation (*T4 Ligase,* Fermentas, Burlington, Canada) of the vector after filling in the complementary overhangs with the Klenow fragment of DNA polymerase I. The construct coding for rgNLS-mCh was obtained by replacing the GFP coding sequence in pBT016Nab2NLSGFPPrA by the mCherry coding sequence and subsequent removal of the PrA coding sequence The coding sequence for mCherry was amplified by PCR (primers: 5'-ctgga tccAT GGTGA GCAAG GGCGA GG and 5'- ctgag gaagc ttTTA CTTGT ACAGC TCGTC CATGC C; uppercase: annealing sequence, lower case: primer overhang, *Phusion* polymerase (Finnzymes, Espoo, Finland) from pcDNA3.1-mCherry (Invitrogen, Carlsbad, CA) and ligated into the *Bam*HI and *Hind*III digested vector. The PrA coding sequence was removed by a *Hind*III and *Nhe*I, digestion. The rgNLS-TC-GFP reporter was constructed by ligation of hybridized oligonucleotides, specifying the tetracysteine motif (TC, CCPGCC [Martin, *et al.* (2005) *Nat. Biotechnol.* **23**:1308-1314]), in the *Bam*HI site between the rgNLS and the GFP coding sequence of pBT016Nab2NLSGFP. The hybridized oligonucleotides were 5'-GATCC ATGTT TTTGA ATTGT TGTCC AGGTT GTTGT ATGGA ACCAA GATCT G and 5'-GATCC AGATC TTGGT TCCAT ACAAC AACCT GGACA ACAAT TCAAA AACAT G.

The construct coding for xGFP was present on pUG34 [Niedenthal, *et al.* (1996) *Yeast* **12**:773-786]. The GFP-cNLS reporter, with a tandem version of the SV40 cNLS (PKKKRKV) located C-terminal of the GFP, was constructed by replacing the *Met25* promoter for a *Gal1* promoter and ligating a cNLS in the multiple cloning site. The *Gal1* promoter was amplified from pYes3/CT (Invitrogen) by PCR and ligated into the *Xba*I and *Sac*I sites of pUG34 (5'-gcatc tagaG GTTTT TTCTC CTTGA CGTTA AAGTA TAGAG G and 5'-gcaga gctcA CGGAT TAGAA GCCGC CGAGC). The cNLS was ligated into the *Bam*HI and *Eco*RI sites as hybridized oligonucleotides (5'-GATCC CCAAA AAAGA AGAGA AAGGT AGATC CAAAA AAGAA GAGAA AGGTA GCTAG CG and 5'-AATTC GCTAG CTACCT TTCTC TTCTT TTTTG GATCT ACCTT TCTCT TCTTT TTTGG G). The TC-motif was inserted in the GFP-cNLS vector by PCR-based mutagenesis (adapted from *Quik Change* protocol, Stratagen, La Jolla, CA) with two opposite primers (5'-ggatg ttgta tggaa ccaga cgtcT CTAGA ATGTC TAAAG GTGAA GAATT ATTTA CTGG and 5'-tggac aacaa ttcat aaaca tGGTT TTTTC TCCTT GACGT TAAAG TATAG AGG) containing the sequence coding for the TC-motif in their overhangs and hybridizing adjacent to the site of integration. Prior to ligation the PCR product was treated with *Dpn*I to digest parental DNA. The construct coding for mCh-cNLS was made by replacing GFP with mCherry and inserting cNLS in pUG36 [Niedenthal, *et al.* (1996) *Yeast* **12**:773-786]. The cNLS was inserted as described for pUG34. The sequence for mCherry was amplified by PCR (5'-ggtct agaAT GGTGA GCAAG GGCGA GG and 5'-gctct agaTT ACTTG TACAG CTCGT CCATG CC) from pcDNA3.1-mCherry and ligated into the *Xba*I site of pUG36. The TC-MBP-cNLS reporter was constructed by replacing in mCh-cNLS the coding sequence for mCherry for maltose binding protein (MBP), tagged with a TC-motif. MBP was amplified by PCR from the *Escherichia coli* genome with two opposite primers (5'-

gctct agaat gttta tgaat tgttg tcccg ggtgt tgtat ggaac caATG AAAAT CGAA GAAGG TAAAC TGGTA ATCTG and 5'-cacgt aggat ccact agtAG TCTGC GCAGC TGCCA GGG). The vector and the PCR product were digested with restriction enzymes *Xba*I and *Bam*HI and the MBP fragment was ligated in the vector. All constructs were confirmed by sequencing.

All experiments were performed in yeast strain BY4742 ([Brachmann, *et al.* (1998) *Yeast* **14**:115-132] *MATα his3Δ1 leu2Δ0 lys2Δ0 ura3Δ0*, Invitrogen), grown in (low fluorescent) synthetic-dropout medium complete (SDC, Sigma-Aldrich, St Louis, MO) at pH 5.4, supplemented with 2% (w/v) glucose and with or without histidine, uracil or leucine. Strain expressing C-terminal GFP-fusion of chromosome encoded *NAB2* (YGL122C), *NAB4* (YOL123W), *PUB1* (YNL016W), *DBP5* (YOR046C), *ASH1* (YKL185W), and *KAP104* (YBR017C) were obtained from Invitrogen and are described in [Huh, *et al.* (2003) *Nature* **425**:686-691]. The strain carrying a deletion of *SHE2* (YKL130C) was obtained from EUROSCARF (YKL130C, acc. nr. Y14980; Germany) and is described in [Winzeler, *et al.* (1999) *Science* **285**:901-906]. The temperature-sensitive Kap104p mutant Kap104-16 was a kind gift from Dr. J.D. Aitchison (Institute for Systems Biology, Seattle, USA) and is described in [Aitchison, *et al.* (1996) *Science* **274**:624-627]. Expression of the TC-GFP-cNLS reporter was induced by growing overnight in synthetic dropout medium without histidine, supplemented with 2% (w/v) raffinose and 0.1% (w/v) galactose (no glucose).

**Immuno-fluorescence labeling**

Cells were grown to $10^7$ cells $ml^{-1}$ and fixed as described (http://www.singerlab.org/protocols, [Long, *et al.* (1995) *RNA* **1:**1071-1078]). Detection of Kap104p was done with a primary antibody raised against Kap104p (Invitrogen, 1:300 (v/v) overnight at 4°C) and a secondary Alexa fluor 633-labeled antibody (Invitrogen, 1:500 (v/v) for 1.5 hr at 20°C).